



HAL
open science

Kerr-lens mode-locked ytterbium-activated orthoaluminate laser

Zhang-Lang Lin, Wen-Ze Xue, Huang-Jun Zeng, Ge Zhang, Peixiong Zhang, Zhenqiang Chen, Zhen Li, Valentin Petrov, Pavel Loiko, Xavier Mateos, et al.

► **To cite this version:**

Zhang-Lang Lin, Wen-Ze Xue, Huang-Jun Zeng, Ge Zhang, Peixiong Zhang, et al.. Kerr-lens mode-locked ytterbium-activated orthoaluminate laser. *Optics Letters*, 2022, 47 (12), pp.3027-3030. 10.1364/OL.460701 . hal-03858737

HAL Id: hal-03858737

<https://hal.science/hal-03858737v1>

Submitted on 19 Nov 2022

HAL is a multi-disciplinary open access archive for the deposit and dissemination of scientific research documents, whether they are published or not. The documents may come from teaching and research institutions in France or abroad, or from public or private research centers.

L'archive ouverte pluridisciplinaire **HAL**, est destinée au dépôt et à la diffusion de documents scientifiques de niveau recherche, publiés ou non, émanant des établissements d'enseignement et de recherche français ou étrangers, des laboratoires publics ou privés.

To be published in Optics Letters:

Title: Kerr-lens mode-locked Yb:(Y,Gd)AlO₃ laser

Authors: Weidong Chen,Zhanglang Lin,Wenze Xue,huangjun zeng,Zhang Ge,Peixiong Zhang,Zhenqiang Chen,Zhen Li,Haifeng Lin,Pavel Loiko,Xavier Mateos,Valentin Petrov,Li Wang

Accepted: 10 May 22

Posted 10 May 22

DOI: <https://doi.org/10.1364/OL.460701>

© 2022 Optica

OPTICA
PUBLISHING GROUP
Formerly OSA

Kerr-lens mode-locked ytterbium-activated orthoaluminate laser

ZHANG-LANG LIN,¹ WEN-ZE XUE,¹ HUANG-JUN ZENG,¹ GE ZHANG,¹
PEIXIONG ZHANG,² ZHENQIANG CHEN,² ZHEN LI,² VALENTIN PETROV,³
PAVEL LOIKO,⁴ XAVIER MATEOS,⁵ HAIFENG LIN,⁶ LI WANG³ AND
WEIDONG CHEN^{1,3,*}

¹Fujian Institute of Research on the Structure of Matter, Chinese Academy of Sciences, Fuzhou, 350002 Fujian, China

²Department of Optoelectronic Engineering, Jinan University, 510632 Guangzhou, China

³Max Born Institute for Nonlinear Optics and Short Pulse Spectroscopy, Max-Born-Str. 2a, 12489 Berlin, Germany

⁴Centre de Recherche sur les Ions, les Matériaux et la Photonique (CIMAP), UMR 6252 CEA-CNRS-ENSICAEN, Université de Caen, 6 Boulevard Maréchal Juin, 14050 Caen Cedex 4, France

⁵Universitat Rovira i Virgili (URV), Física i Cristal·lografia de Materials (FICMA), 43007 Tarragona, Spain

⁶College of Physics and Optoelectronic Engineering, Shenzhen University, 518118 Shenzhen, China

*Corresponding author: chenweidong@fjirsm.ac.cn

Received XX Month XXXX; revised XX Month, XXXX; accepted XX Month XXXX; posted XX Month XXXX (Doc. ID XXXXX); published XX Month XXXX

We report on the first Kerr-lens mode-locked laser based on an Yb³⁺-doped perovskite-type orthoaluminate crystal exploiting two different principal light polarizations. The Yb:(Y,Gd)AlO₃ laser delivers soliton pulses as short as 32 fs at 1067 nm with an average output power of 328 mW, a pulse repetition rate of ~84.6 MHz for *E* || *a* polarization. For the orthogonal *E* || *b* polarization, 33-fs pulses are generated at 1057 nm with an average output power of 305 mW. Power scaling to a maximum average output power reaching 2.07 W is achieved at the expense of longer pulse duration (72 fs for *E* || *b*), corresponding to an optical efficiency of 43.9% and a peak power of 303 kW.
© 2022 Optical Society of America

<http://dx.doi.org/10.1364/OL.99.099999>

Mode-locked (ML) solid-state Yb-lasers emitting few-optical-cycle pulses in the spectral range of ~1 μm represent a hot topic in the field of ultrafast optics. Compared to ML Ti:sapphire lasers operating near 800 nm, they feature the following advantages: i) extremely low quantum defect resulting in very high optical efficiency and reduced thermal issues; ii) power-scalable operation using cost-effective and commercially available high-power fiber-coupled InGaAs laser diodes as pump sources; and iii) compact configurations suitable for robust integration [1].

Recently, efforts towards exploiting the broadband gain spectra of Yb³⁺-doped disordered crystals for few-optical-cycle pulse generation resulted in entering the sub-20 fs time domain. Y. Wang *et al.* passed this mark for the first time in 2021 using Yb:CaGdAlO₄ aluminate as a gain medium and generating 17.8 fs pulses at 1118 nm with an average output power of only 26 mW (optical efficiency $\eta_{\text{opt}} = 3.3\%$) via Kerr-lens mode-locking (KLM) [2]. Subsequently, 17 fs pulses at 1080 nm were emitted from a similar

KLM laser based on an isostructural aluminate crystal, Yb:CaYAlO₄, albeit with a lower average output power of 18 mW and η_{opt} of only 0.47% [3]. These results indicate quite clearly the existing trade-off between ultimate pulse shortening and output power scalability. To overcome this limitation, a pump scheme allowing one to reduce the quantum defect was employed in a KLM Yb:CaGdAlO₄ laser delivering soliton pulses as short as 22 fs at 1040.7 nm with an average output power of 729 mW and a reasonably high $\eta_{\text{opt}} = 25\%$ [4]. Ordered host crystals normally possess higher thermal conductivity and are more suited for high output powers/optical efficiencies but classical crystals such as YAG do not offer such broad spectral gain. For instance, a diode-pumped KLM Yb:YAG laser generating 35 fs pulses at 1060 nm with an average output power of 107 mW was demonstrated in 2011 [5]. A shorter pulse duration of 27 fs at 1028 nm for an average output power of 3.3 W was obtained from a KLM thin-disk Yb:YAG laser albeit at an optical efficiency of only 1.05% [6].

Ytterbium (Yb³⁺)-doped yttrium orthoaluminate, Yb:YAlO₃ (shortly Yb:YAP), is a structurally ordered laser crystal belonging to the orthorhombic class (sp. gr. *Pnma*, perovskite-type structure). It is very promising for the development of high-power 1 μm lasers due to a combination of excellent thermo-mechanical and spectroscopic properties [7-10]. In particular, it possesses relatively high thermal conductivity, $\kappa_a = 7.1$, $\kappa_b = 8.3$ and $\kappa_c = 7.6$ Wm⁻¹K⁻¹ (values along the crystallographic axes for 5 at.% Yb³⁺ doping) [11], which is beneficial for power scalable operation under pumping with commercial high-power InGaAs laser diodes emitting at ~0.98 μm. YAP is optically biaxial and its intrinsic birefringence together with the polarization anisotropy of the Yb³⁺ ion emission properties leads to a linearly polarized laser emission, suppressing thermally induced depolarization losses inherent to cubic laser crystals such as Yb:YAG. The first investigation on its passive mode-locking was reported in 2008: using a Semiconductor Saturable Absorber Mirror (SESAM), 225 fs pulses were generated at 1041 nm with an

average output power of 0.8 W [12]. Subsequently, the same group reported on power scaling of the SESAM ML Yb:YAlO₃ laser using a novel off-axis pumping scheme yielding 140 fs pulses at 1009.7 nm with an average output power of 4 W [7]. However, no sub-100 fs ML Yb:YAP laser operation has been reported, yet.

Very recently, we developed a Yb³⁺-doped yttrium-gadolinium “mixed” orthoaluminate crystal exhibiting compositional disorder, i.e., Yb:Y_{1-x}Gd_xAlO₃ or Yb:(Y,Gd)AlO₃ [13]. The estimated mean thermal conductivity of this material is $\sim 6.3 \text{ Wm}^{-1}\text{K}^{-1}$ [14, 15], indicating a high potential for power scalable laser operation. By implementing a SESAM for starting and stabilizing the soliton pulse shaping, we achieved 43 fs pulses from a diode-pumped Yb:(Y,Gd)AlO₃ laser [15]. The superior thermo-optical properties and preliminary mode-locking results motivated us to further explore the potential of the Yb:(Y,Gd)AlO₃ crystal for few-optical-cycle generation via soft-aperture KLM.

A high-quality Yb³⁺-doped Y_{0.85}Gd_{0.10}Yb_{0.05}AlO₃ crystal with an Yb³⁺ doping level of 5.65 at.% was grown by the conventional Czochralski method. The laser operation was investigated using an X-shaped astigmatically compensated standing-wave cavity. The schematic of the laser cavity and pumping geometry is presented in Fig. 1.

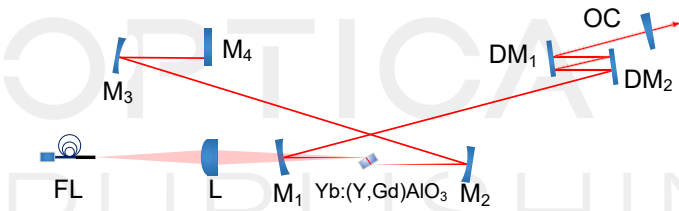


Fig. 1. Schematic of the Yb:(Y,Gd)AlO₃ laser. FL: fiber laser; L: spherical focusing lens ($f = 75 \text{ mm}$); M₁ – M₃, dichroic concave mirrors; M₄: flat rear mirrors; DM₁ and DM₂: dispersive mirrors; OC: output coupler.

An uncoated 3-mm thick laser crystal was cut from the as-grown bulk, oriented for light propagation along the crystallographic *c*-axis (*c*-cut) with an aperture of 4 (a) \times 4 (b) mm² (sp. gr. *P_{mma}*). It was mounted in a water-cooled copper holder (coolant temperature: 19°C) and placed at Brewster’s angle between two concave dichroic folding mirrors M₁ and M₂ (radius of curvature: RoC = -100 mm) with the minimum loss condition fulfilled for both the pump and laser wavelengths and polarizations. One arm of the laser cavity was completed by an additional concave mirror M₃ (RoC = -100 mm) and a flat rear mirror M₄. The other cavity arm was terminated by a pair of flat dispersive mirrors (DMs) and a flat-wedged output coupler (OC). DM₁ and DM₂ were implemented to compensate the intracavity group delay dispersion (GDD) and balance the self-phase modulation (SPM) induced by the Kerr nonlinearity of the laser crystal for soliton pulse shaping. All DMs had a negative GDD of -200 fs^2 per bounce. A continuous-wave, spatially single-mode fiber laser emitting a nearly diffraction-limited (M^2 of ~ 1.04) linearly polarized beam was used as a pump source. Its emission wavelength was locked at 979 nm with a spectral linewidth (full width at half maximum, FWHM) of $\sim 0.1 \text{ nm}$. The pump beam was focused into the laser crystal by a spherical lens ($f = 75 \text{ mm}$) yielding a beam waist radius of $15.4 \mu\text{m} \times 28.6 \mu\text{m}$ in the sagittal and tangential planes, respectively. By rotating the crystal, we were able to set the laser polarization ($\mathbf{E} \parallel \mathbf{a}$ or $\mathbf{E} \parallel \mathbf{b}$).

The Yb:(Y,Gd)AlO₃ laser was initially characterized for light polarization $\mathbf{E} \parallel \mathbf{b}$ corresponding to stronger pump absorption ($>99\%$ in ML operation) and an OC transmittance (T_{OC}) of 4.5%. The KLM regime was investigated at an incident pump power of 3.05 W by applying four bounces (single pass) on the flat DMs giving a round-trip GDD of -1600 fs^2 . In order to discriminate the CW and KLM regimes, the laser cavity was aligned close to the edge of the stability region through translating the folding mirror (M₂) by several hundreds of micrometers away from the pump mirror (M₁), which resulted in a significant drop of the CW output power. KLM operation could be initiated by a slight knock on the OC or translating the flat rear mirror M₄. This led to an abrupt increase of the output power from 0.535 to 1 W. The spectrum of the femtosecond pulses was centered at 1053.2 nm with a FWHM of 23.2 nm by assuming a sech²-shaped spectral profile, see Fig. 2(a).

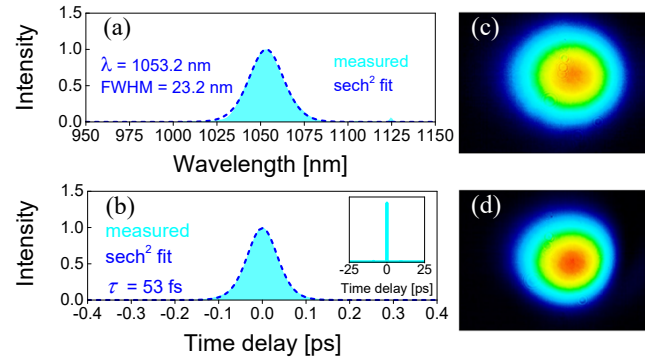


Fig. 2 KLM Yb:(Y,Gd)AlO₃ laser with $T_{\text{OC}} = 4.5\%$ ($\mathbf{E} \parallel \mathbf{b}$): (a) Optical spectrum and (b) autocorrelation trace. *Inset* in (b): simultaneously measured long-scale (50 ps) autocorrelation trace. (c,d) Far-field beam profiles: transition from (c) CW to (d) KLM regime.

The recorded background-free intensity autocorrelation trace can be almost perfectly fitted with a sech²-shaped temporal profile, giving an estimated pulse duration of 53 fs (FWHM), see Fig. 2(b). The corresponding time-bandwidth product (TBP) of 0.332 was only slightly above the Fourier-transform-limited value (0.315). A long-scale intensity autocorrelation scan of 50 ps confirmed single-pulse steady-state ML, see the inset in Fig. 2(b). The total cavity length was $\sim 1.8 \text{ m}$, resulting in a pulse repetition rate of $\sim 83.2 \text{ MHz}$. The peak output power reached $\sim 200 \text{ kW}$. The calculated peak on-axis intracavity intensity in the laser crystal was $\sim 1.23 \text{ TW/cm}^2$. Such a high intensity should lead to a noticeable modification of the spatial mode. This was indeed confirmed by monitoring the far-field beam profiles with a camera placed at $\sim 1.6 \text{ m}$ away from the OC. The shrinking of the far-field beam diameter from $2.53 \times 2.23 \text{ mm}^2$ to $2.17 \times 2.01 \text{ mm}^2$, as shown in Fig. 2(c) and (d), indicated a strong soft-aperture Kerr-lens effect and self-focusing inside the laser crystal.

The pulse duration could be reduced by applying lower T_{OC} of 2.5% while maintaining the same total round-trip negative GDD. Notably shorter pulses of 38 fs were obtained at 1056 nm with a $\sim 31 \text{ nm}$ spectral FWHM. In this case, the corresponding TBP was 0.317, again very close to the Fourier-transform-limit. The average output power was 0.763 W (peak power: $\sim 212.1 \text{ kW}$) at a pulse repetition rate of $\sim 83.3 \text{ MHz}$, yielding a peak on-axis laser intensity in the laser crystal of $\sim 2.37 \text{ TW/cm}^2$. The shortest pulse duration for laser polarization $\mathbf{E} \parallel \mathbf{b}$ was achieved by further reducing the

transmittance of the OC to 1.6%. Soliton pulses as short as 33 fs were generated at 1057 nm with a spectral FWHM of 36 nm, as shown in Fig. 3. The TBP was 0.319, only slightly above the Fourier limit for sech^2 -shaped pulses. The peak output power of the laser pulses was 97.8 kW corresponding to an estimated peak on-axis laser intensity of $\sim 1.72 \text{ TW/cm}^2$ in the crystal.

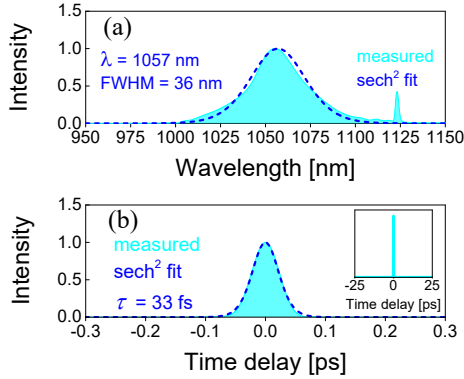


Fig. 3. KLM Yb:(Y,Gd)AlO₃ laser with $T_{OC} = 1.6\%$ ($\mathbf{E} \parallel \mathbf{b}$): (a) Optical spectrum and (b) autocorrelation trace. *Inset* in (b): long-scale (50 ps) autocorrelation trace.

A maximum output power of 305 mW at $\sim 83.2 \text{ MHz}$ was obtained for an incident pump power of 3.1 W, corresponding to an optical efficiency of 9.84%. A sharp satellite peak is observed at 1123 nm, which originates from the unmanaged intracavity GDD at the long-wave spectral wing and the non-optimized spectral reflectivity of the cavity mirrors. This phenomenon has been already observed in ML Yb:CaGaAlO₄ lasers [16], and explained by F. Druon *et al.* [17]. It could be improved by properly managing the total intracavity GDD over the full spectral band of the ML laser.

Table 1. Characteristics^a of the KLM Yb:(Y,Gd)AlO₃ laser vs Output Coupling for Laser Polarization $\mathbf{E} \parallel \mathbf{b}$

T_{OC} [%]	P_{pump} [W]	P_{out} [W]	η_{opt} [%]	λ_c [nm]	$\Delta\lambda$ [nm]	$\Delta\tau$ [fs]
1.6	3.1	0.305	9.84	1057	36	33
2.5	3.2	0.763	23.8	1056	30.9	38
4.5	3.05	1	32.8	1053.2	23.2	53
7.5	3.9	1.4	35.9	1053.5	20.7	58
10	4.72	2.07	43.9	1050.1	16	72

^a T_{OC} – output coupler transmittance, P_{pump} – incident pump power, P_{out} – average output power, η_{opt} – optical efficiency refers to incident pump power, λ_c – central laser wavelength, $\Delta\lambda$ – spectral bandwidth (FWHM), $\Delta\tau$ – pulse duration (FWHM).

Power scalable operation for the laser polarization $\mathbf{E} \parallel \mathbf{b}$ was investigated by increasing the output coupling to $T_{OC} = 7.5\%$ and 10%. The pump power was adjusted for achieving single-pulse mode-locking with the highest average output power, as well as the highest optical efficiency. Table 1 summarizes the results for various T_{OC} values. The average output power of the KLM Yb:(Y,Gd)AlO₃ laser was easily scaled by cranking up the pump power at the expense of the pulse duration. The maximum average output power reached 2.07 W at an incident pump power of 4.72 W. This corresponded to a longer pulse duration of 72 fs, still in the sub-100 fs time range, and a relatively high optical efficiency of 43.9%.

The spectrum of the ML laser experienced a slight blue-shift to 1053.5 nm ($T_{OC} = 7.5\%$) and 1050.1 nm ($T_{OC} = 10\%$), as can be expected for a three-level laser system with reabsorption.

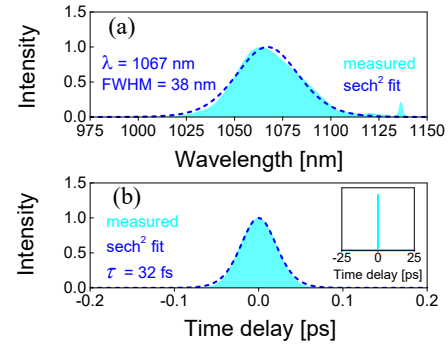


Fig. 4. KLM Yb:(Y,Gd)AlO₃ laser with $T_{OC} = 1.6\%$ ($\mathbf{E} \parallel \mathbf{a}$): (a) Optical spectrum and (b) autocorrelation trace. *Inset* in (b): long-scale (50 ps) autocorrelation trace.

The KLM operation of the Yb:(Y,Gd)AlO₃ laser was also studied for the other available light polarization, $\mathbf{E} \parallel \mathbf{a}$, characterized by lower pump absorption ($< 75\%$ in ML operation). As expected, the shortest pulses with ultimate mode-locking stability were achieved with the 1.6% OC. A maximum average output power of 328 mW was obtained at an incident pump power of 3.75 W and a pulse repetition rate of 84.6 MHz. This corresponded to an optical efficiency of 8.7%. The pulse characteristics are shown in Fig. 4. The laser spectrum had a FWHM of 38 nm at 1067 nm by assuming a sech^2 -shaped spectral profile, see Fig. 4(a). The pulse duration was assessed from the recorded background-free intensity autocorrelation trace which is shown in Fig. 4(b). The curve can be almost perfectly fitted with a sech^2 -shaped temporal profile yielding a deconvolved FWHM of 32 fs. The TBP was thus 0.320, slightly above the Fourier-transform-limit. A longer time window (50-ps) autocorrelation scan confirmed single-pulse mode-locking without post- or pre-pulses, see the inset in Fig. 4(b). The peak output power reached $\sim 106.6 \text{ kW}$ and the estimated peak on-axis laser intensity in the crystal amounted to $\sim 1.87 \text{ TW/cm}^2$.

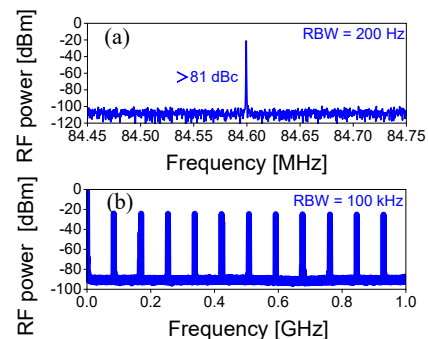


Fig. 5. RF spectra of the KLM Yb:(Y,Gd)AlO₃ laser ($\mathbf{E} \parallel \mathbf{a}$): (a) Fundamental beat note, RBW = 200 Hz; (b) 1-GHz span with RBW of 100 kHz. RBW: resolution bandwidth.

Figure 5 shows the recorded radio-frequency (RF) spectrum of the steady-state pulse train of the shortest pulses for light

polarization $E \parallel a$. The recorded narrow-band fundamental beat note exhibited a very high extinction ratio of 81 dBc above carrier at 84.6 MHz, see Fig. 5(a). This, together with the uniform harmonic beat notes on a 1-GHz frequency span indicates highly stable KLM operation without any Q-switching instabilities or multi-pulsing, see Fig. 5(b).

Power scaling of the KLM laser for light polarization $E \parallel a$ was also investigated by increasing the output coupling in the range of $T_{OC} = 2.5\% - 7.5\%$, cf. Table 2 summarizing the achieved output characteristics. Due to the relatively low pump absorption compared to $E \parallel b$, the maximum incident pump power reached 6 W for achieving single-pulse mode locking with higher average output power and optical efficiency. The maximum average output power reached 1.72 W at an incident pump power of 6 W for a pulse duration of 51 fs. This, corresponded to a lower optical conversion of 28.7% compared to $E \parallel b$.

Table 2. Characteristics^a of the KLM Yb:(Y,Gd)AlO₃ laser vs Output Coupling for Laser Polarization $E \parallel a$

T_{OC} [%]	P_{pump} [W]	P_{out} [W]	η_{opt} [%]	λ_c [nm]	$\Delta\lambda$ [nm]	$\Delta\tau$ [fs]
1.6	3.75	0.328	8.7	1067	38	32
2.5	3.3	0.498	15.1	1065.3	33.3	37
4.5	6	1.24	20.7	1053.5	25.3	50
7.5	6	1.72	28.7	1051.8	22.9	51

^a T_{OC} – output coupler transmittance, P_{pump} – incident pump power, P_{out} – average output power, η_{opt} – optical efficiency refers to incident pump power, λ_c – central laser wavelength, $\Delta\lambda$ – spectral bandwidth (FWHM), $\Delta\tau$ – pulse duration (FWHM).

To conclude, “mixed” ytterbium-doped yttrium-gadolinium orthoaluminate crystal, Yb:(Y,Gd)AlO₃, with compositional disorder, represents an attractive laser material for generation of ultrashort (sub-100 fs) pulses with moderate to high average output powers (up to the watt-level) from Kerr-lens mode-locked solid-state lasers. Owing to its good thermal properties, as well as intense and broad emission bands for polarized light, two regimes of KLM operation were successfully exploited: i) targeting the shortest pulse duration, 32 fs pulses were generated at 1067 nm with an average output power of 328 mW at a repetition rate of 84.6 MHz for light polarization $E \parallel a$ using low output coupling ($T_{OC} = 1.6\%$), ii) targeting the maximum average output power and laser efficiency, the KLM laser delivered 2.07 W at 1050.1 nm at the expense of longer pulse duration (72 fs) corresponding to an optical efficiency of 43.9% for light polarization $E \parallel b$ employing high output coupling ($T_{OC} = 10\%$). To the best of our knowledge, this is the first demonstration of Kerr-lens mode-locking employing Yb³⁺-doped orthorhombic perovskite-type aluminate crystals. Our results pave the way towards the development of high-power (>10 W) KLM ytterbium orthoaluminate lasers pumped by cost-efficient spatially multi-mode InGaAs laser diodes. Heavily-doped Yb:YAlO₃-type crystals also look promising for KLM thin-disk lasers at $\sim 1 \mu\text{m}$

Funding. National Natural Science Foundation of China (61975208, 61905247, 61875199, U21A20508, 51972149, 51872307, 61935010); Sino-German Scientist Cooperation and Exchanges Mobility Program (M-0040); National Key Research and Development Program of China (2021YFB3601504); Key-Area Research and Development Program of Guangdong Province

(2020B090922006); Agencia Estatal de Investigación (PID2019-108543RB-I00).

Acknowledgment. Xavier Mateos acknowledges the Serra Hünter program.

Disclosures. The authors declare no conflicts of interest

Disclosures. Data underlying the results presented in this paper are not publicly available at this time but may be obtained from the authors upon reasonable request.

References

1. D. E. Spence, J. M. Dudley, K. Lamb, W. E. Sleat, and W. Sibbett, *Opt. Lett.* **19**, 481 (1994).
2. A. Schlatter, B. Rudin, S. C. Zeller, R. Paschotta, G. J. Spuhler, L. Krainer, N. Haverkamp, H. R. Telle, and U. Keller, *Opt. Lett.* **30**, 1536 (2005).
3. U. Keller, *Appl. Phys. B* **100**, 15 (2010).
4. Y. Feng, T. P. Lamour, H. Ostapenko, R. A. McCracken, O. Mandel, D. Weise, and D. T. Reid, *Opt. Lett.* **46**, 5429 (2021).
5. Y. Wang, X. Su, Y. Xie, F. Gao, S. Kumar, Q. Wang, C. Liu, B. Zhang, B. Zhang, and J. He, *Opt. Lett.* **46**, 1892 (2021).
6. J. Ma, F. Yang, W. Gao, X. Xiaodong, X. Jun, D. Shen, and D. Tang, *Opt. Lett.* **46**, 2328 (2021).
7. F. Labaye, V. J. Wittwer, M. Hamrouni, N. Modsching, E. Cormier, and T. Südmeyer, *Opt. Express* **30**, 2528 (2022).
8. S. Uemura, and K. Torizuka, *Jpn. J. Appl. Phys.* **50**, 010201 (2011).
9. J. Drs, J. Fischer, N. Modsching, F. Labaye, V. J. Wittwer, and T. Südmeyer, *Opt. Express* **29**, 35929 (2021).
10. A. Rudenkov, V. Kisel, A. Yasukevich, K. Hovhannesian, A. Petrosyan, and N. Kuleshov, *Devices and Methods of Measurements* **11**, 179 (2020)
11. K. Hovhannesian, M. Derdzian, A. Yeganyan, V. Kisel, A. Rudenkov, N. Kuleshov, and A. Petrosyan, *J. Contemp. Phys.* **55**, 131 (2020).
12. J. Petit, B. Viana, P. Goldner, J. P. Roger, and D. Fournier, *J. Appl. Phys.* **108**, 123108 (2010)
13. G. Boulon, Y. Guyot, H. Canibano, S. Hraiech, and A. Yoshikawa, *J. Opt. Soc. Am. B* **25**, 884 (2008).
14. R. Aggarwal, D. Ripin, J. Ochoa, and T. Fan, *J. Appl. Phys.* **98**, 103514 (2005).
15. V. E. Kisel, S. V. Kurilchik, A. S. Yasukevich, S. V. Grigoriev, S. A. Smirnova, and N. V. Kuleshov, *Opt. Lett.* **33**, 2194 (2008).
16. H. Tan, R. Wang, P. Zhang, H. Yin, Z. Li, and Z. Chen, *J. Synth. Cryst.* **50**, 2013 (2021).
17. R. Gaumé, B. Viana, D. Vivien, J. P. Roger, and D. Fournier, *Appl. Phys. Lett.* **83**, 1355 (2003).
18. W. Z. Xue, Z. L. Lin, H. J. Zeng, G. Zhang, P. Zhang, Z. Chen, Z. Li, V. Petrov, P. Loiko, X. Mateos, H. Lin, Y. Zhao, L. Wang, and W. Chen, *Opt. Express* **30**, 11825 (2022).
19. Y. Zaouter, J. Didierjean, F. Balembois, G. L. Leclin, F. Druon, P. Georges, J. Petit, P. Goldner, and B. Viana, *Opt. Lett.* **31**, 119 (2006).
20. P. Sévillano, P. Georges, F. Druon, D. Descamps, and E. Cormier, *Opt. Lett.* **39**, 6001 (2014).

References

1. D. E. Spence, J. M. Dudley, K. Lamb, W. E. Sleat, and W. Sibbett, "Nearly quantum-limited timing jitter in a self-mode-locked Ti:sapphire laser," *Optics Letters* **19**, 481-483 (1994).
2. A. Schlatter, B. Rudin, S. C. Zeller, R. Paschotta, G. J. Spuhler, L. Krainer, N. Haverkamp, H. R. Telle, and U. Keller, "Nearly quantum-noise-limited timing jitter from miniature Er:Yb:glass lasers," *Optics Letters* **30**, 1536-1538 (2005).
3. U. Keller, "Ultrafast solid-state laser oscillators: a success story for the last 20 years with no end in sight," *Applied Physics B* **100**, 15-28 (2010).
4. Y. Feng, T. P. Lamour, H. Ostapenko, R. A. McCracken, O. Mandel, D. Weise, and D. T. Reid, "Towards a space-qualified Kerr-lens mode-locked laser," *Optics Letters* **46**, 5429-5432 (2021).
5. Y. Wang, X. Su, Y. Xie, F. Gao, S. Kumar, Q. Wang, C. Liu, B. Zhang, B. Zhang, and J. He, "17.8 fs broadband Kerr-lens mode-locked Yb:CALGO oscillator," *Optics Letters* **46**, 1892-1895 (2021).
6. J. Ma, F. Yang, W. Gao, X. Xiaodong, X. Jun, D. Shen, and D. Tang, "Sub-five-optical-cycle pulse generation from a Kerr-lens mode-locked Yb:CaYAlO₄ laser," *Optics Letters* **46**, 2328-2331 (2021).
7. F. Labaye, V. J. Wittwer, M. Hamrouni, N. Modsching, E. Cormier, and T. Südmeyer, "Efficient few-cycle Yb-doped laser oscillator with Watt-level average power," *Optics Express* **30**, 2528-2538 (2022).
8. S. Uemura, and K. Torizuka, "Sub-40-fs Pulses from a Diode-Pumped Kerr-Lens Mode-Locked Yb-Doped Yttrium Aluminum Garnet Laser," *Jpn J Appl Phys* **50** (2011).
9. J. Drs, J. Fischer, N. Modsching, F. Labaye, V. J. Wittwer, and T. Südmeyer, "Sub-30-fs Yb:YAG thin-disk laser oscillator operating in the strongly self-phase modulation broadened regime," *Optics Express* **29**, 35929-35937 (2021).
10. A. Rudenkov, V. Kisel, A. Yasukevich, K. Hovhannesyanyan, A. Petrosyan, and N. Kuleshov, "High Power SESAM Mode-Locked Laser Based on Yb³⁺:YAlO₃ Bulk Crystal," *Devices and Methods of Measurements* **11**, 179 (2020). (2020).
11. K. Hovhannesyanyan, M. Derdzyan, A. Yeganyan, V. Kisel, A. Rudenkov, N. Kuleshov, and A. Petrosyan, "Single Crystals of YAP:Yb for Ultra Short Pulse Lasers," *Journal of Contemporary Physics (Armenian Academy of Sciences)* **55**, 131-136 (2020).
12. J. Petit, B. Viana, P. Goldner, J.-P. Roger, and D. Fournier, "Thermomechanical properties of Yb³⁺ doped laser crystals: Experiments and modeling," *J Appl Phys* **108**, 123108 (2010).
13. G. Boulon, Y. Guyot, H. Canibano, S. Hraiech, and A. Yoshikawa, "Characterization and comparison of Yb³⁺-doped YAlO₃ perovskite crystals (Yb: YAP) with Yb³⁺-doped Y₃Al₅O₁₂ garnet crystals (Yb:YAG) for laser application," *JOSA B* **25**, 884-896 (2008).
14. R. Aggarwal, D. Ripin, J. Ochoa, and T. Fan, "Measurement of thermo-optic properties of Y₃Al₅O₁₂, Lu₃Al₅O₁₂, YAlO₃, LiYF₄, LiLuF₄, BaY₂F₈, KGd(WO₄)₂, and KY(WO₄)₂ laser crystals in the 80 - 300 K temperature range," *J Appl Phys* **98**, 103514 (2005).
15. V. E. Kisel, S. V. Kurilchik, A. S. Yasukevich, S. V. Grigoriev, S. A. Smirnova, and N. V. Kuleshov, "Spectroscopy and femtosecond laser performance of Yb³⁺:YAlO₃ crystal," *Optics Letters* **33**, 2194-2196 (2008).
16. H. Tan, R. Wang, P. Zhang, H. Yin, Z. Li, and Z. Chen, "Growth and properties of Gd³⁺/Yb³⁺ co-doped yttrium aluminate crystals," *Journal of Synthetic Crystals* **50**, 2013 (2021).
17. R. Gaumé, B. Viana, D. Vivien, J.-P. Roger, and D. Fournier, "A simple model for the prediction of thermal conductivity in pure and doped insulating crystals," *Appl Phys Lett* **83**, 1355-1357 (2003).
18. W.-Z. Xue, Z.-L. Lin, H.-J. Zeng, G. Zhang, P. Zhang, Z. Chen, Z. Li, V. Petrov, P. Loiko, X. Mateos, H. Lin, Y. Zhao, L. Wang, and W. Chen, "Diode-pumped SESAM mode-locked Yb:(Y,Gd)AlO₃ laser," *Optics Express* **30**, 11825-11832 (2022).
19. Y. Zaouter, J. Didierjean, F. Balembos, G. L. Leclin, F. Druon, P. Georges, J. Petit, P. Goldner, and B. Viana, "47-fs diode-pumped Yb³⁺:CaGdAlO₄ laser," *Optics Letters* **31**, 119-121 (2006).
20. P. Sévillano, P. Georges, F. Druon, D. Descamps, and E. Cormier, "32-fs Kerr-lens mode-locked Yb:CaGdAlO₄ oscillator optically pumped by a bright fiber laser," *Optics Letters* **39**, 6001-6004 (2014).